Improvement the rituximab production by O-GlcNAcylation using Thiamet G

Hye Yeon Kim

Department of Medical Science

The Graduate School, Yonsei University

Improvement the rituximab production by O-GlcNAcylation using Thiamet G

Hye Yeon Kim

Department of Medical Science

The Graduate School, Yonsei University

Improvement the rituximab production by O-GlcNAcylation using Thiamet G

Directed by Professor Joo Young Kim

The Master's Thesis
submitted to the Department of,
The Graduate School of Yonsei University
in partial fulfillment of the requirements for the degree of
Master of Medical Science

Hye Yeon Kim

June 2019

This certifies that The Master's Thesis of Hye Yeon Kim is approved.

Thesis Supervisor: Joo Young Kim

Thesis Committee Member #1: Jong Sun Kim

Thesis Committee Member #2: Kyoung Hee Jun

The Graduate School

Yonsei University

June 2019

ACKNOWLEDGEMENTS

우선, 저에게 과분한 애정과 관심으로 지도해주신 김주영 교수님께 감사 드립니다. 2년동안 교수님의 학문적 호기심과 열정을 직접 옆에서 보고 배울 수 있어 영광이었습니다. 그리고 부족한 저를 믿어주시어 스스로 연구를 이끌어 나갈 수 있도록 길을 틔워주신 점 무엇보다 감사 드리며 앞으로도 잊지 않고 그에 보답할 수 있도록 열심히 노력하겠습니다.

또한, 바쁘신 시간에도 불구하고 예심과 본심을 거치는 기간 동안 애정 어린 관심으로 지도해주신 김종선 교수님과 전경희 교수님께 감사 드립니다. 심사 기간을 통해 혼자서는 생각하지 못했던 부분들을 다시 한번 새로이 생각해보는 기회가 되었고, 연구의 완성도를 높일 수 있었던 소중한 시간이었습니다.

그리고 역사 깊은 약리학 교실에서 훌륭한 교수님들 밑에서 가르침과 지도를 받으며 학위를 받을 수 있어 영광이었습니다. 도움을 주신 약리학 교실의 박경수 교수님, 이민구 교수님, 김철훈 교수님, 지헌영 교수님, 김형범 교수님께 감사 드립니다.

그 외 도움을 주신 약리학교실 분들께 진심으로 감사 드리며 여러분의 도움이 없었더라면 혼자서 이루지 못했을 것이라 생각합니다. 그 중에서도 2년 동안 가장 의지하며 도움을 준 나래 언니에게 가장 큰 감사함을 전하고 싶습니다. 그리고, 언제나 아낌없이 실험적, 정신적 도움을 주신 엄소원 선생님께도 감사함을 전하고 싶습니다. 또한, 힘들고 어려운 점이 많았을 텐데도 불만 없이 열심히 잘 따라준 명수에게도 고마움을 전하고 싶습니다. 이외 항상 즐거운 에너지를 주고받은 이민구 교수님, 지헌영 교수님 랩 구성원 분들께도 감사인사 드립니다.

마지막으로, 언제나 저의 꿈을 믿어주고 아낌없이 지원해주시며 제가 마음껏 날개를 펼칠 수 있도록 뒤에서 든든히 저를 지켜주시는 부모님께 가장 감사 드립니다. 앞으로 평생 그 사랑에 보답할 수 있도록 노력하겠습니다. 그리고, 잘 챙겨주지 못해 미안한 동생 일도 에게도 감사함과 미안함을 전합니다.

TABLE OF CONTENTS

LIST OF FIGURES

ABSTRACT

Improvement the rituximab production by O-GlcNAcylation using Thiamet G

Hye Yeon Kim

Department of Medical Science
The Graduate School, Yonsei University

(Directed by Professor Joo Young Kim)

O-Glycosylation occurs in recombinant proteins produced by CHO cells, but this phenomenon has not been studied extensively. Here, we report that rituximab is an O-linked N-acetyl-glucosaminylated (O-GlcNAcylated) protein.

The abundance of serine and threonine in rituximab, which are sites for O-GlcNAcylation, led us to develop a method to increase production using thiamet G, an inhibitor of O-GlcNAcase (OGA). The production of rituximab doubled with OGA inhibition and decreased with O-GlcNAc transferase (OGT) inhibition. The radioactive isotope experiment revealed that the degradation of rituximab was reduced when thiamet G was treated. O-GlcNAc-specific antibody confirmed the increased O-GlcNAcylation with thiamet G and metabolic labelling using N-acetyl-azido-glucosamine (Ac4GlcNAz) confirmed that rituximab is an O-GlcNAcylated protein. Protein mass analysis revealed that serine 7, 12, and 14 of the light chain

were O-GlcNAcylated. S12A mutation of the light chain decreased rituximab stability and failed to increase production with thiamet G. This revealed that serine 12 is an important factor for regulation of rituximab production. Cytotoxicity and thermal stability assays confirmed that there were no differences in the biological and physical properties of rituximab produced by thiamet G treatment. Therefore, thiamet G treatment improves the production of rituximab without significantly altering its function. Meanwhile, we found that serine 12 of light chain also conserved in anti-PD1 antibodies and showed increased production by thiamet G.

Our results suggest that O-GlcNAcylation of serine12 by treatment with thiamet G could be used as a way to increase the production of rituximab and antibodies with serine 12.

Key words: rituximab, O-GlcNAc, production yield, thiamet G, ADCC, CDC, thermal stability

Improvement the rituximab production by O-GlcNAcylation using Thiamet G

Hye Yeon Kim

Department of Medical Science
The Graduate School, Yonsei University

(Directed by Professor Joo Young Kim)

I. INTRODUCTION

Rituximab is a monoclonal antibody that recognises the B cell surface protein CD20[1] and causes B cell depletion. It was developed as a therapeutic agent for non-Hodgkin lymphoma, which is a type of blood cancer[2] and led to the development of various therapeutic monoclonal antibodies against CD20. Since the patent for rituximab has expired, several pharmaceutical companies are producing rituximab biosimilars.

Antibody drugs produced in CHO cells undergo post-translational modifications (PTMs),[3,4] of which glycosylations are the most common modifications.[3] Proteins can be modified by N- or O-glycosylation, where the glycans bind to the asparagine residue or the oxygen atom of an amino acid residue in a protein, respectively.[5] Many studies have focused on N-glycans attached to the CH2 domain of the Fc region of antibodies.[6] As a result, N-glycans have emerged as an important factor that determines the quality of antibodies, including their therapeutic effect,[7,8] half-life[9,10] and immune reaction.[11]

On the other hand, the O-glycans are far more complicated and have diverse types

than the N-glycans.[12] The most well-known O-glycosylation is the mucin type O-glycosylation, in which the reducing end of N-acetyl-galactosamine (GalNAc) is linked to the Ser/Thr residue. After initiation by GalNAc, the chain is extended by galactosamine, glucosamine, fucose, sialic acid, and other sugars to form a complex and diverse structure.[13] In addition, there are diverse types of O-glycan structures in which N-acetyl-glucosamine (GlcNAc), fucose, galactose, and mannose are also bound.[14] O-GlcNAc is also a well understood type of O-glycosylation,[15] in which the addition of a GlcNAc to Ser/Thr residues of nuclear and cytosolic proteins is catalysed by O-GlcNAc transferase (OGT), and the reverse reaction is catalysed by O-linked N-acetyl-glucosaminidase (OGA).[16] O-GlcNAc has been reported to augment protein stability.[15] For instance, O-GlcNAcylation increases the stability and protein levels of Sp1, Nup62, and FOXO1.[17-19] Furthermore, O-GlcNAc on peptides decreases their ubiquitination and inhibits proteasomal degradation.[20]

In this study, we focused on O-glycosylation of rituximab, which is abundant in serine and threonine residues compared to other therapeutic monoclonal antibodies. Analysis of several antibody sequences using the O-GlcNAc prediction tool, suggested that rituximab has several sites for O-GlcNAc residues with high threshold.[21] We confirmed the increased O-GlcNAcylation of rituximab in the presence of an OGA inhibitor, thiamet G[22] by western blot using O-GlcNAc specific antibody. When the rituximab producing cells were treated with thiamet G, the product yield doubled. We also confirmed that O-GlcNAcylation of rituximab has no significant effect on biological activities and physical properties of the cells with respect to cell death, efficacy and thermal stability of the antibody. Therefore, we propose that O-GlcNAcylation by thiamet G treatment could be an improved method for the production of rituximab without significantly altering its characteristics.

II. MATERIALS AND METHODS

1. Cells and transfection

Chinese Hamster Ovary cell line (CHO-K1) and Human B-lymphoma RAMOS were purchased from ATCC. Cells were maintained in RPMI-1640 medium supplemented with 10% fetal calf serum and 1% penicillin/streptomycin at 37 ℃, 5% CO_2. Polyethylenimine (25 kDa) reagent (Polysciences, 23966-1, Inc, PA18976) was used for transient transfection in CHO-K1 cells.

2. Reagents and solutions

For cell cultures, RPMI-1640 medium (ThermoFisher Scientific, 11875093), fetal bovine serum (FBS) (ThermoFisher Scientific, 26140079), Penicillin-Streptomycin (ThermoFisher Scientific, 15140122), and Trypsin-EDTA 0.05% solution (ThermoFisher Scientific, 25300062) were used.

For inhibitor treatment, thiamet G (Sigma-Aldrich, SML0244)[22] and OSMI-1 (Sigma-Aldrich, SML1621)[23] were used. For immunoblotting, NaCl (Sigma-Aldrich, S7653), Triton X-100 (Sigma-Aldrich, T8787), Glycerol (Sigma-Aldrich, G5516), EDTA (USB Corporation, 15694), Tris ultrapure (Duchefa Biochemie, T1501), Complete proteinase inhibitors (Roche Applied Science), HCl (FUJIFILM Wako Pure Chemical Corporation, 084-05425), NaOH (FUJIFILM Wako Pure Chemical Corporation, 196-05375), BCA Protein Assay Kit (ThermoFisher Scientific, 23227), 5 × Tricine-SDS sample buffer (KOMA Biotech Inc., KTR020-5), and pre-cast 4-12% gradient SDS-PAGE gels (KOMA Biotech Inc., KG5012) were used.

For metabolic labeling of O-GlcNAc, Ac4GlcNAz (88903; ThermoFisher Scientific, Waltham, MA USA), Phosphine-biotin (13581; Cayman chemical, Michigan, USA) were used.

3. Antibodies and fluorescent dyes

For immunoblots, HRP-conjugated anti-O-linked N-acetyl-glucosamine antibody (RL2, Abcam, ab20199) and HRP-conjugated anti-human IgG specific antibody (JACKSON Lab, 109-035-003) were used. For fluorescent dyes, FITC-conjugated anti-Human IgG antibody (Abcam, ab81051) was used.

4. Generation of antibody producing CHO cells

To generate cells stably expressing rituximab, obinutuzumab, nivolumab and pembrolizumab, we produced lentiviruses expressing heavy or light chain of the antibodies, GNT3 or MAN2A. DNA sequence of rituximab, nivolumab and pembrolizumab were retrieved from US patent 7381560, the light and heavy chain nucleotide sequence was synthesised by Bioneer Corporation and inserted into the viral vector pLenti6. The production of obinutuzumab was as previously described.[24] The light and heavy chain were transfected into HEK cells to produce lentivirus particles. Then both light and heavy chain expressing lentiviruses were used to infect CHO-K1 cells, which were selected in growth medium containing 10 μg/mL puromycin (Invivogen, ant-pr-1) and 10 μg/mL blasticidin S (Sigma, 15205) for a week. CHO-K1 cells were transduced with LVX-GNT-Hygro and LVX-MAN2A-Bleo viruses and selected with 500 μg/mL hygromycin (AG Scientific) and 100 μg/mL zeocin (Invitrogen), respectively for a week. The resulting CHO-GE cell was transduced with lentiviruses expressing heavy and light chain of obinutuzumab and selected with 10 μg/mL puromycin and 10 μg/mL blasticidin S (BIOMAX, SMB001-100). Overexpression of myc-rGnT3 was confirmed by western blot analysis with anti-myc antibody (Santa Cruz, SC-40; Supplementary Figure 2B) and transcriptional expression of rGnT3 and Man3 was confirmed with RT-PCR analysis. The selected cells were multiplied to 10 plates of 100 mm cell culture dishes and treated with sodium butyrate to eliminate methylated DNA and to increase the expression level of the antibody. The cell media cultured for 10 days was collected for purification of

secreted antibody using protein A beads (GE Healthcare Life Sciences). The concentration of the antibody was measured with SDS-PAGE and Coomassie staining with BSA as a standard.

5. Production and purification of rituximab

Rituximab producing cells grown to 80% confluency in RPMI-1640 medium containing 10% FBS and 10 μg/mL ciprofloxacin (Sigma-Aldrich, 17850) were washed twice with PBS and refreshed with EX-CELL® CD CHO Serum-Free medium (Sigma-Aldrich) containing 1 mM sodium butyrate. Conditioned media containing monoclonal antibody was obtained by further incubation for 14 days at 30℃ in 5% CO_2, 95% air. Antibodies were purified by affinity chromatography using protein A-Sepharose bead (GE Healthcare Life Sciences). Buffer change and concentration was performed by ultrafiltration with Amicon® Ultra-2 (Millipore, UFC801024), before filter sterilisation and storage. The antibodies were analysed by SDS-PAGE and Coomassie blue staining, and their concentration was quantified relative to BSA band intensity for 0.2, 0.4, 0.8, 1.6, and 3.2 μg of BSA used as standard.

6. Immunoblotting for rituximab

Rituximab stable cells were seeded into 6-well plates at 1×10^6 cells/well and incubated at 37℃ overnight in an incubator enriched with 5% CO_2. On the following day, the medium was changed to serum free RPMI-1640 medium. Thiamet G and OSMI-1 were added to described doses. The supernatant was harvested and stored at −70 ℃. Cells were lysed in lysis buffer (150 mM NaCl, 5 mM Na-EDTA, 10% glycerol, 20 mM Tris-HCl pH 8.0, 0.5 % Triton X-100, and complete proteinase inhibitor). Protein concentration was quantified using Bradford Protein Assay according to the manufacturer's instructions. The lysates and supernatant were mixed with 5 × Tricine-SDS sample buffer, and separated on pre-cast 4-12 % gradient SDS-

PAGE gels. HRP-conjugated anti-human, anti-mouse, anti-O-GlcNAc antibodies were used for immunoblotting. Protein L(Thermo Fisher, 1189) was used for immunoprecipitation.

7. Metabolic labelling by azido-sugar.

CHO_Rituximab cells were seeded into T75 flask and incubated at 37℃ in an incubator enriched with 5% CO_2 atmosphere incubator overnight. Next day, we treated 50 μM Ac4GlcNAz, 50 μM thiamet G to cells. Conditioned media containing rituximab were obtained by further incubation for 3 days at 37℃ in 5% CO_2/95% air. Antibodies were purified via affinity chromatography using protein A-Sepharose bead (GE Healthcare Life Sciences). Buffer-changed and concentration was conducted by ultrafiltration with Amicon® Ultra-2 before filter-sterilization and storage.

Purified rituximab were reacted with equivalent volume of 500 μM phosphine-biotin for 16 hours at room temperature. Reaction products were immunoblotted with streptavidin-HRP and stripped membrane was re-blotted with anti-human IgG and anti-mouse IgG specific antibodies.

8. Immunoblotting for transient expression

For transient transfection, CHO-K1 cells were seeded into 6-well plates at 1×10^6 cells/well and incubated at 37℃ overnight in an incubator enriched with 5% CO_2. Then, the cells were transfected using polyethylenimine for 6 hours, the medium changed to serum free RPMI-1640 medium the following day and incubated for a further 3 days. Then the supernatant was harvested and stored at −70°C and the cells were lysed in lysis buffer. Protein concentration was quantified using Bradford Protein Assay according to the manufacturer's instructions. The lysates and supernatant were mixed with 5 × Tricine-SDS sample buffer and separated on pre-cast 4-12% gradient SDS-PAGE gels. HRP-conjugated anti-human, anti-mouse, and

anti-O-GlcNAc were used for immunoblotting.

9. Protein stability assay using 35S Labeling of rituximab.

CHO-rituxan stable cells grown in 100 mm plates. Methionine depletion was carried out with incubation in a methionine-free DMEM for 2 hours before labeling. Then cells were supplemented with 0.1 mCi/ml [^{35}S] Methionine (PerkinElmer Life Sciences) for 1 hour at 37℃. The cells were then washed with serum free DMEM and incubated with 8 ml of serum free DMEM media for 0, 2, 5 and 8 hours. At each time, media was collected and cells were lysised then the antibody in media and lysates (1 mg of protein) were precipitated with protein A agarose bead (50% slurry 30 μL, ThermoScientific), separated by 4%~12% SDS-PAGE, and visualized by autoradiography.

10. In-gel digestion with trypsin and extraction of peptides

Protein bands from SDS-PAGE gels were excised and in-gel digested with trypsin according to established procedures (Bahk et al., 2004). In brief, protein bands were excised from stained gels and cut into pieces. The gel pieces were washed for 1 hour at room temperature in 25 mM ammonium bicarbonate buffer, pH 7.8, containing 50 % (v/v) acetonitrile (ACN). Following the dehydration of gel pieces in a centrifugal vacuum concentrator (Biotron, Inc., Incheon, Korea) for 10 min, gel pieces were rehydrated in 50 ng of sequencing grade trypsin solution (Promega, Madison, WI, USA). After incubation in 25 mM ammonium bicarbonate buffer, pH 7.8, at 37℃ overnight, the tryptic peptides were extracted with 5 μL of 0.5% formic acid (FA) containing 50% (v/v) ACN for 40 min with mild sonication. The extracted solution was concentrated using a centrifugal vacuum concentrator. Prior to mass spectrometric analysis, the peptides solution was subjected to a desalting process using a reversed-phase column (Gobom et al., 1999). In brief, after an equilibration step with 10 μL of 5% (v/v) formic acid, the peptides solution was loaded on the

column and washed with 10 μL of 5% (v/v) formic acid. The bound peptides were eluted with 5 μL of 70% ACN with 5% (v/v) formic acid.

11. Identification of proteins by LC-MS/MS

LC–MS/MS analysis was performed through nano ACQUITY UPLC and LTQ-orbitrap-mass spectrometer (Thermo Electron, San Jose, CA). The column used BEH C18 1.7 μm, 100 μm ×100 mm column (Waters, Milford, MA, USA). The mobile phase A for the LC separation was 0.1% formic acid in deionized water and the mobile phase B was 0.1% formic acid in acetonitrile. The chromatography gradient was set up to give a linear increase from 10% B to 40% B for 21 min, from 40% B to 95% B for 7 min, and from 90% B to 10% B for 10 min. The flow rate was 0.5 μL/min. For tandem mass spectrometry, mass spectra were acquired using data-dependent acquisition with full mass scan (300-2000 m/z) followed by MS/MS scans. Each MS/MS scan acquired was an average of one microscans on the LTQ. The temperature of the ion transfer tube was controlled at 160℃ and the spray was 1.5-2.0 kV. The normalized collision energy was set at 35% for MS/MS. The individual spectra from MS/MS were processed using the SEQUEST software (Thermo Quest, San Jose, CA, USA) and the generated peak lists were used to query in house database using the MASCOT program (Matrix Science Ltd., London, UK). We set the modifications of methionine, cysteine, methylation of arginine, and phosphorylation of serine, threonine, and tyrosine for MS analysis and tolerance of peptide mass was 2 Da. MS/MS ion mass tolerance was 1 Da, allowance of missed cleavage was 1, and charge states (+1, +2, +3) were taken into account for data analysis. We took only significant hits as defined by MASCOT probability analysis.

12. Measurement of complement cell cytotoxicity and antibody mediated cell death

To analyse cell death, 5×10^4 cells/well of RAMOS cells were plated in 12-well

plates and treated with 1 μM calcein-AM (Invitrogen, C3100MP) for 30 min at 37℃ for staining viable cells. Cells were re-suspended into 100 μL medium and treated with the indicated dose of antibody (0.1, 0.3, 1, 3, and 10 μg/mL) for 10 min. For measurement of complement-dependent cytotoxicity assay, rabbit complement MA was added to a quarter of the total volume and incubated at 37℃ in CO_2 incubator for 2 hours. For antibody-dependent cell-mediated cytotoxicity assay, the same method as with complement-dependent cytotoxicity assay was used. After antibody treatment, purified peripheral blood mononuclear cells (PBMC) (PBMC:RAMOS = 5:1) were added and incubated at 37℃ in CO_2 incubator for 4 hours. The % of cell lysis (% of cells losing fluorescence among 10,000 counted total cells) was calculated by FACSVerse (BD Biosciences) and FlowJo software.

13. Purification of PBMC cells

PBMC was purified using blood from healthy donors who voluntarily participated in our study according to IRB procedure approved by the committee of Yonsei IRB board. All procedures were approved by IRB (#4-2016-0600). Briefly, 4 mL of blood was centrifuged at 1600 ×g to collect cells, which were re-suspended in 8 mL PBS and loaded onto 4 mL Ficoll (Sigma-Aldrich, Histopaque-1077) and centrifuged at 400 ×g for 35 min at 20℃ to separate white blood cells from red blood cells. The white blood cell layer was collected in fresh tubes and washed three times (centrifuged at 300 ×g for 10 min) with RPMI-1640 medium to completely remove the platelet. Purified PBMC cells were counted and incubated in RPMI-1640 medium until use.

14. Circular dichroism measurement

The circular dichroism (CD) spectra were recorded on a Chirascan plus (Applied Photophysics) equipment with a temperature control system in a continuous mode. Thermal denaturation experiments were performed using a heating rate of 1 ℃/min.

Thermal scan data were collected from 20℃ to 90℃ in 2 mm path length cuvettes with protein concentration of 0.2 mg/mL. The CD spectra were measured at a wavelength of 218 nm.

15. Cell viability assay

Cell viability rates were measured by using Cell Titer-Glo Luminescent Cell Viability Assay (Promega, G7570) in 96-well, opaque-wall microplates (Corning Costar, CLS3595). Rituximab stable cells were seeded in 96-well plates (25000 cells per well) in RPMI medium. After an overnight incubation, cells were treated with varying concentrations of thiamet G for conditioned incubation times. Total ATP content as an estimate of total number of viable cells was measured by a microplate luminometer (Centro XS3 LB960).

16. Statistical analysis

Data are presented as the mean ± standard error of the mean. Statistical analysis was performed with Student's t-test or with analysis of variance (ANOVA), followed by Tukey's multiple comparison and one-way or two-way ANOVA tests using the GraphPad Prism software package (version 5.0), as appropriate. $P < 0.05$ was considered statistically significant.

III. RESULTS

1. O-GlcNAcase inhibition by thiamet G doubles the production of rituximab

O-GlcNAcylation is known to regulate protein stability by reducing the ubiquitination of elongating peptides and inhibiting proteasomal degradation.[19] We developed a method to improve the yield of rituximab by increasing the O-GlcNAcylation of the antibody expressed in CHO cells. To determine the effect of inhibiting OGA on rituximab production, stable antibody producing CHO cells were treated with the OGA inhibitor thiamet G. Cells were incubated in chemically defined CHO medium with or without 50 μM thiamet G for 2 weeks in a CO_2 incubator at 30 ℃. Rituximab was purified from the culture media using protein A affinity resin and the concentration of antibodies was determined by Bradford assay and Coomassie blue gel staining. The yield of rituximab was calculated as mass per media volume. We found that the yield of rituximab was two-fold more with thiamet G treatment compared to no treatment (Fig. 1A).

In order to determine if thiamet G changed the rituximab production, thiamet G was treated with various concentrations to confirm the improved production (Fig. 1B and C). The highest production was observed at 50 μM of thiamet G treatment.

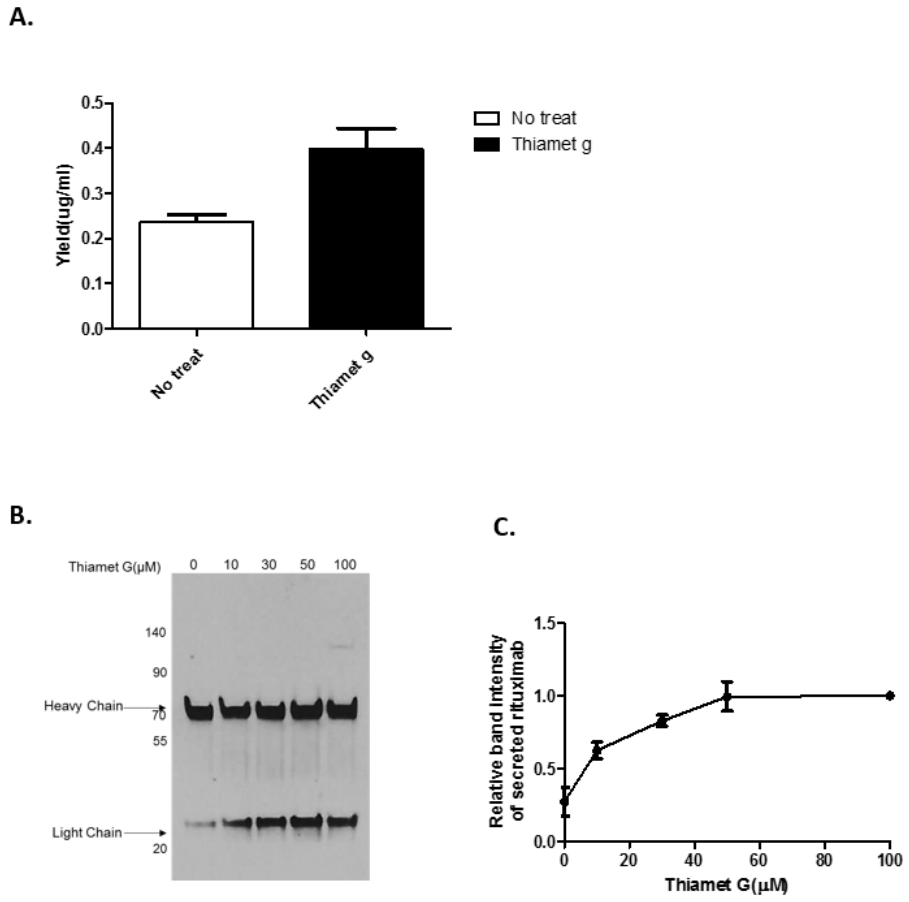

Figure 1. Rituximab production is improved by thiamet G treatment. (A) Purified rituximab's production yields were calculated. Add Serum free RPMI to 100 mm plate rituximab stable cell line and treated 50 μM thiamet G. After incubation at 30℃ for 2 weeks, purified rituximab with protein A. Antibody concentration was measured by Bradford method and quantification of PAGE gel analysis with Coomassie blue staining. (B) Thiamet G concentration-dependent increase in the production of rituximab. Equal numbers of rituximab producing stable cells were seeded to culture plates and treated with thiamet G (0, 10, 30, 50, 100 μM). After 48

hours, equal volumes of the culture medium (15 μL) was used for immunoblotting with HRP-conjugated anti-human IgG and anti-mouse IgG antibodies. (C) Summary graph after quantification of band intensity of immunoblot depicted in B.

2. Confirmation of rituximab production changed by O-GlcNAc-related inhibitors

In order to obtain direct evidence of the effect of thiamet G treatment, we investigated the time-dependent effect of thiamet G on rituximab production. As shown in Figure 2A and B, we confirmed the time-dependent (24, 48 and 72 hour) increase in rituximab production upon thiamet G treatment.

Next, we determined the effect of inhibiting O-GlcNAcylation on the production of rituximab. We treated the rituximab producing CHO cells with an OGT inhibitor OSMI-1 (Fig. 2C and D). Treatment with 50 μM OSMI-1 decreased the production of rituximab at all time points (24, 48 and 72 hour). These results together demonstrate that the regulation of O-GlcNAcylation affects the production and yield of rituximab.

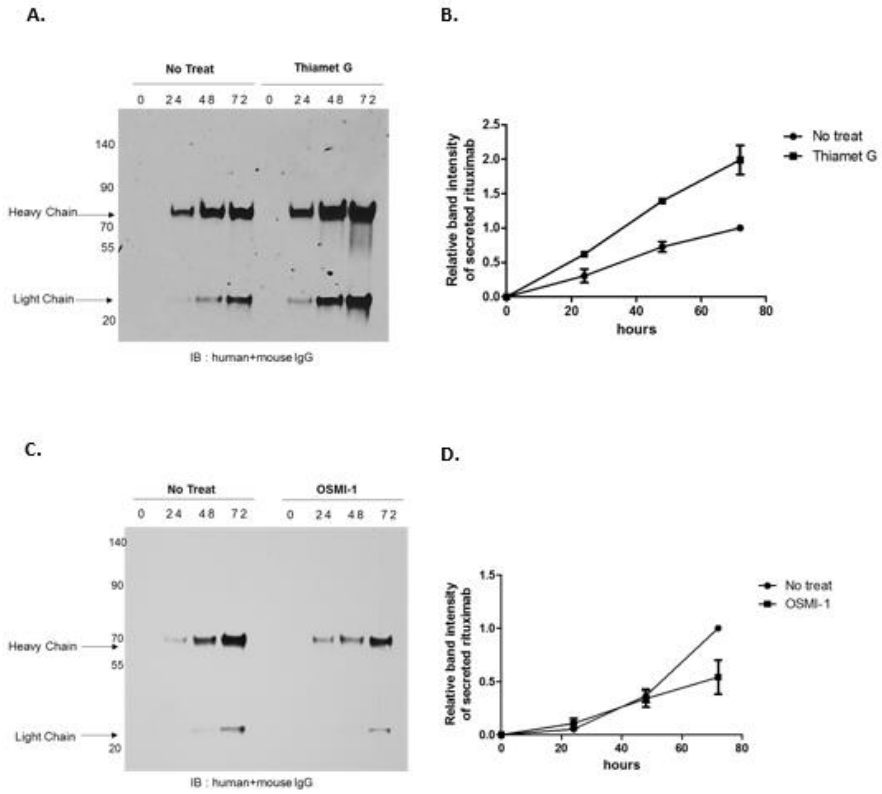

Figure 2. Comparison of rituximab production after inhibition of OGA using thiamet G (A) Increase in rituximab production over time (0, 24, 48, 72 hour) after treatment of rituximab producing stable cells with 50 μM thiamet G. Equal numbers of rituximab producing stable cells were seeded to culture plates and treated with thiamet G. After each time points, equal volumes of the culture medium (15 μL) was used for immunoblotting with HRP-conjugated anti-human IgG and anti-mouse IgG antibodies. (B) Summary graph after quantification of band intensity of immunoblot depicted in A. (C) Decrease in rituximab production over time (0, 24, 48, 72 hour) after treating rituximab producing stable cells with 50 μM OSMI-1. At each time

point, equal volumes of the cultured medium (15 μL) was loaded and immunoblotted with HRP-conjugated anti-human IgG and anti-mouse IgG antibodies. (D) Summary graph of the quantification of bands in the immunoblot shown in C.

3. Rituximab is an O-GlcNAcylated protein

To confirm the enhanced O-GlcNAcylation of rituximab upon thiamet G treatment, we performed immunoblot assay using anti-O-GlcNAc antibody.[25,26] The purified rituximab was separated by polyacrylamide gel electrophoresis (PAGE) under reducing and non-reducing conditions, confirmed by coomassie blue staining and quantified with immunoblotting (Fig. 3A, B). The horse radish peroxidase (HRP)-conjugated anti-O-GlcNAc antibody (RL2) was used for the immunoblot assay because rituximab is a chimeric antibody. Increased levels of O-GlcNAcylations of rituximab was observed with thiamet G treatment compared to untreated cells and Mabthera® (Roche). Increased O-GlcNAcylated proteins in thiamet G treated CHO cell lysate was used as a positive control for O-GlcNAcylation of the protein.

Next, we performed metabolic labelling of O-GlcNAc by azido-sugar (Fig. 3C). Rituximab stable cells were treated 50 μM Ac4GlcNAz and then incubated for 3 days. After purification of rituximab, staudinger reaction was carried out with phosphine-biotin. O-GlcAz conjugated with biotin were subjected to immunoblot with streptavidin-HRP. O-GlcNAc was labelled in light and heavy chains. These results suggest that rituximab is O-GlcNAc modified protein.

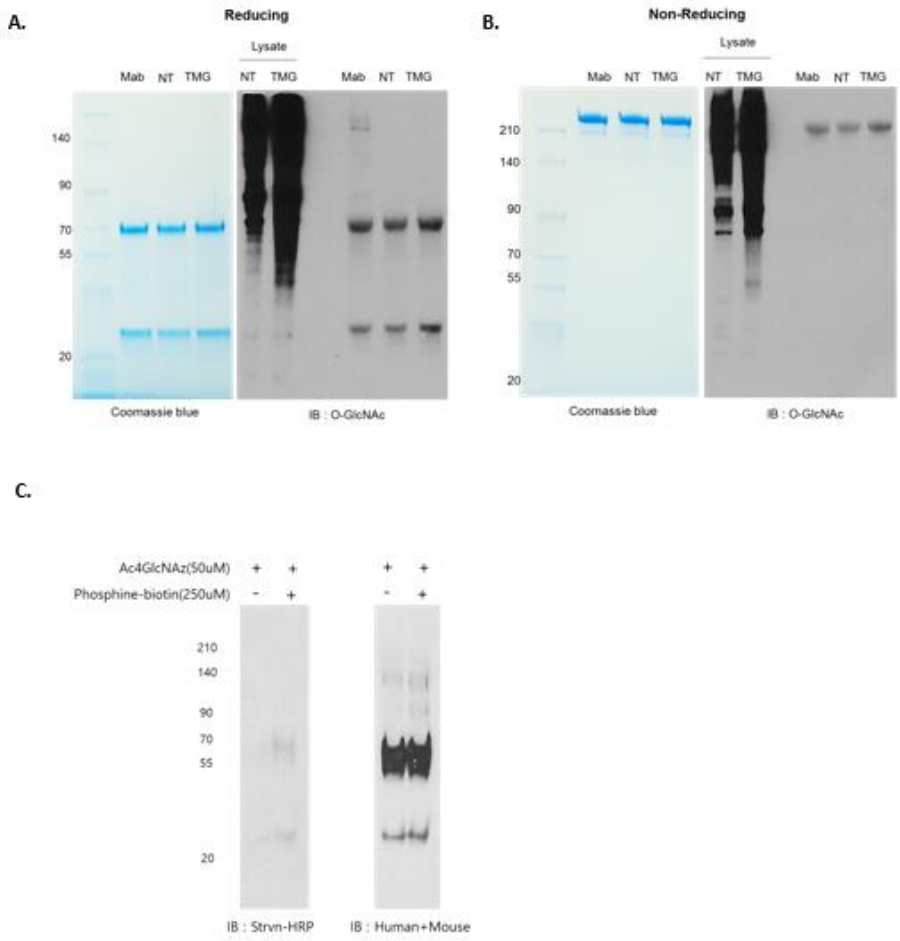

Figure 3. Rituximab is an O-GlcNAcylated protein. (A) O-GlcNAcylation of rituximab is increased upon thiamet G treatment in reducing condition. (B) O-GlcNAcylation of rituximab is increased upon thiamet G treatment in non-reducing condition. Left panel: purified antibody (1 μg) was quantified using PAGE separation and coomassie blue staining. Right panel: thiamet G treated CHO cell lysate (10 μg) was used as a control for anti-O-GlcNAc antibody. Purified rituximab (4 μg) were immunoblotted with HRP-conjugated anti-O-GlcNAc antibody under reducing and

non-reducing conditions. Right panel: purified antibody (1 μg) was quantified using PAGE separation and Coomassie blue staining in reducing and non-reducing conditions. NT: not treated; TMG: thiamet G-treated; Mab: Mabthera® (Roche). (C) Metabolic labelling of rituximab by N-azido-acetyl-glucosamine (Ac4GlcNAz). Detection of rituximab-O-GlcNAz-biotin. Rituximab stable cells were treated with 50 μM Ac4GlcNAz for 3 days. Purified rituximab was incubated with phosphine-FLAG overnight at 16℃. Reaction products were subjected to immunoblot with streptavidin-HRP. Stripped membrane was immunoblotted with human and mouse IgG specific-HRP conjugated antibody.

4. Thiamet G treatment inhibits the degradation of rituximab.

In order to investigate the degradation time of rituximab when thiamet G treated, we performed a radioactive isotope experiment. In Fig. 4A, no treated and thiamet G treated rituximab stable cells were incubated for 1 hour in ^{35}S methionine media. Serum free media was changed, and lysates were harvested at 0, 2, 5, and 8 hour, and immunoprecipitation were performed by protein A. Rituximab in no treated cells almost depleted at 8 hour, while thiamet G treated cells maintained a protein level. Fig. 4B shows the quantification of heavy chain's band intensity. These results suggest that thiamet G treatment to rituximab stable cells inhibits the degradation of rituximab.

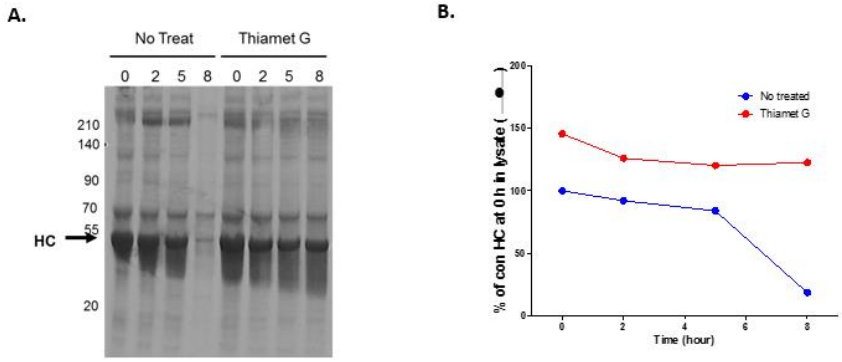

Figure 4. Thiamet G inhibits the degradation of rituximab. (A) Labeling of ^{35}S methionine of rituximab stable cells. Incubate ^{35}S methionine DMEM media for 1 hour and change the media to serum free DMEM. Harvested lysate were subjected to immunoprecipitation with protein A and loaded to SDS-PAGE gels. Gel was visualized by autoradiography. (B) Graph shows the quantification of relative intensity of the heavy chain bands.

5. Mass spectrometry analysis of rituximab light chain detected the O-GlcNAcylation on rituximab

To clearly elucidate the site of O-GlcNAcylated on rituximab, we conducted a mass spectrometry analysis by LTQ-Orbitrap-mass spectrometer to find the O-GlcNAc site of the rituximab. We found O-GlcNAc modification (HexNAc (1) at m / z 203) on serine 7, 12, 14 of rituximab light chain (Fig.5A)

O-GlcNAc has been reported to be involved in protein stability.[15] It is known that proteins such as SP1, FOXO1 are caused by O-GlcNAc by non-specific binding of OGT.[15] O-GlcNAc on protein decreases ubiquitination and proteasomal degradation is inhibited.[19] To test the effect of each O-GlcNAcylation site on yield and stability of rituximab, we constructed alanine substitution mutants of each identified serine

site in the light chain. We transiently expressed the mutants of light chain in CHO-K1 cells incubated at 30 ℃ for 5 days. Among these, S12A mutant of the light chain showed severely reduced expression compared to the WT and other mutants (Fig. 5B).

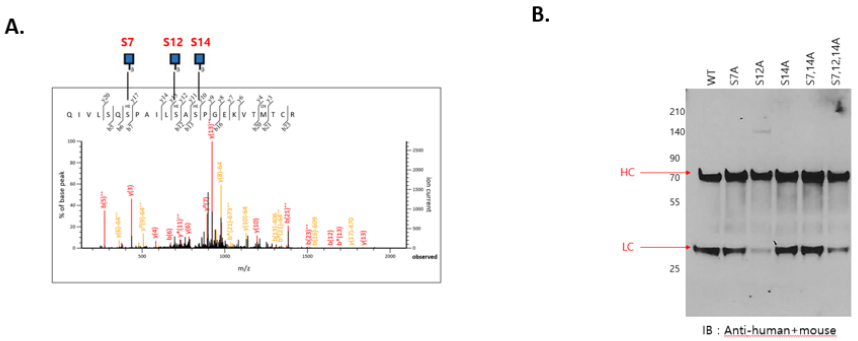

Figure 5. O-GlcNAcylation of seine 12 on rituximab light chain is required for rituximab stability. (A) Rituximab light chain is O-GlcNAcylated at serine 7, serine 12, and serine 14. An MS/MS spectrum was generated from LTQ-orbitrap-mass spectrometer. (B) Each Mutant of light chain serine 7, 12, 14 were transfected to CHO-K1 cells with Heavy chain and incubated at 30˚C for 14 days. Harvested sup were subjected to immunoblot with human and mouse IgG specific-HRP conjugated antibody.

6. O-GlcNAcylation of rituximab light chain serine 12 regulate the productivity of rituximab

To confirm that O-GlcNAcylation on serine 12 affects the productivity of rituximab upon thiamet G treatment, we generated light chain S12A rituximab stable CHO cells and observed the time-dependent and dose-dependent effect of thiamet G treatment on S12A rituximab production. As shown in Figure 6A and B, we confirmed that the production of S12A rituximab was not affected by thiamet G at any time point (24, 48 and 72 hour) and thiamet G concentrations (0, 10, 30, 50 and 100 μM).

Collectively, these results suggest that rituximab is an O-GlcNAcylated protein and its productivity can be regulated by the OGA inhibitor, thiamet G. Furthermore, the Ser7, Ser12 and Ser14 of the light chain of rituximab were O-GlcNAcylated and Ser12 might be a critical O-GlcNAcylation site that contributes to thiamet G-dependent enhanced production.

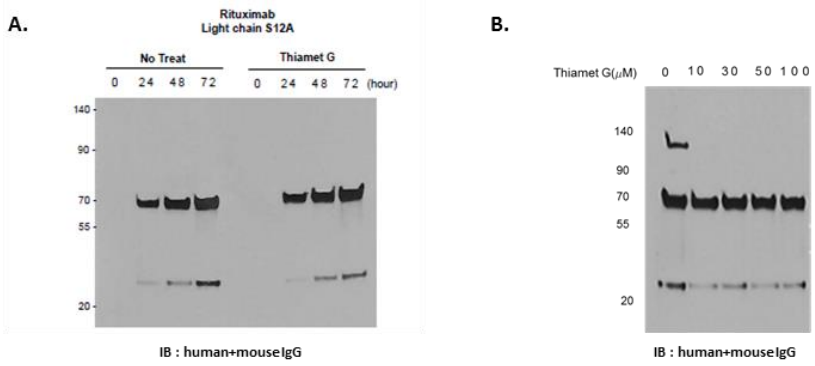

Figure 6. Thiamet G does not improve the production of S12A mutants. (A) S12A rituximab production over time (0, 24, 48, 72 hour) after treatment of rituximab producing stable cells with 50 μM thiamet G. Equal numbers of rituximab producing stable cells were seeded to culture plates and treated with thiamet G. After each time points, equal volumes of the culture medium (15 μL) was used for immunoblotting

with HRP-conjugated anti-human IgG and anti-mouse IgG antibodies. (B) Thiamet G concentration-independent production of S12A rituximab. Equal numbers of rituximab producing stable cells were seeded to culture plates and treated with thiamet G (0, 10, 30, 50, 100 μM). After 48 hours, equal volumes of the culture medium (15 μL) was used for immunoblotting with HRP-conjugated anti-human IgG and anti-mouse IgG antibodies.

7. O-GlcNAcylation of rituximab does not affect the biological activities and thermal stability of the antibody

The alteration of N-glycans change the characteristics of monoclonal antibodies.[27,28] Therefore, to investigate whether O-GlcNAcylation of rituximab affects its efficacy, we compared the biological activities of rituximab produced with or without thiamet G treatment using flow cytometry analysis. For biological activity testing, complement-dependent cytotoxicity (CDC) (Fig. 7A) and antibody-dependent cell-mediated cytotoxicity (ADCC) (Fig. 7B) were measured. Both biological activities were similar between rituximab produced by untreated and thiamet G treated cells. Obinutuzumab with little CDC and high ADCC activity was used as a control for this analysis.[29]

It is known that glycans affect the thermal stability of antibodies.[30,31] In order to determine if O-GlcNAcylation of rituximab affects its thermal stability, melting temperature (Tm) was measured using circular dichroism spectra at 218 nm (Fig. 7C). No differences were observed in the Tm values of rituximab produced by untreated (79℃) and thiamet G-treated (80℃) cells. Mabthera® (77℃) was used as a control for the analysis. These results demonstrate that O-GlcNAcylation of rituximab has little influence on antibody efficacy and protein thermal stability.

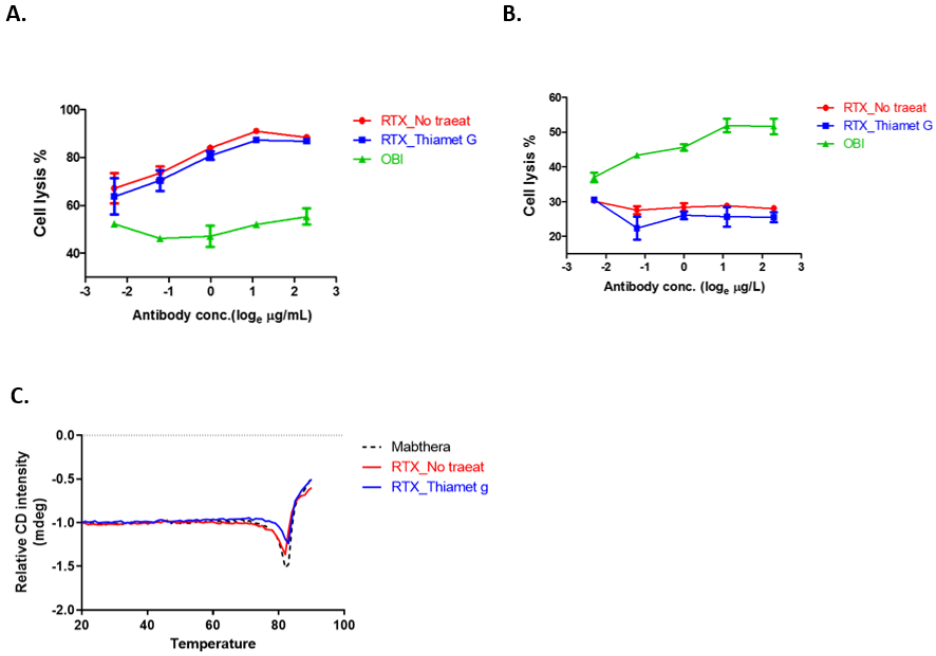

Figure 7. Evaluation of the biological and physical properties of rituximab produced by thiamet G treated cells. Complement-dependent cytotoxicity (A) and antibody-dependent cell-mediated cytotoxicity (B) were assessed using flow cytometry to confirm dose dependency of antibodies (0.1, 0.3, 1, 3, 10 μg/mL). (C) Circular dichroism (CD) spectra of melting temperature (Tm) measurement of antibodies. The CD values measured at 218 nm are plotted against temperature ranging from 20˚C to 90˚C.

8. The effect of thiamet G concentrations and incubation time on cell viability.

CellTiter-Glo was used to investigate the effect of thiamet G treatment on cell viability in rituximab stable cells. Fig. 9A, rituximab stable cells were treated with 0. 50, 100, 200, 300, 400 and 500 μM of thiamet G. After incubation at 30 ° C for 4 days, luminescence of live cells were measured. Compared with 0 M , cell viability was slightly increased at 50μM, and there were no difference in cell viability at concentrations above 100μM.

In Fig. 9B, the cell viability of thiamet G-treated rituximab cells were measured during the 14 days of incubation period. Cell viability was observed on the day after treatment with thiamet G at 0, 10, 50, 100, 200 μM at 30 ℃. As a result, the viability was slightly higher than that at 0μM at the concentration of ~ 50μM, and was similar to 0 μM at the concentrations above.

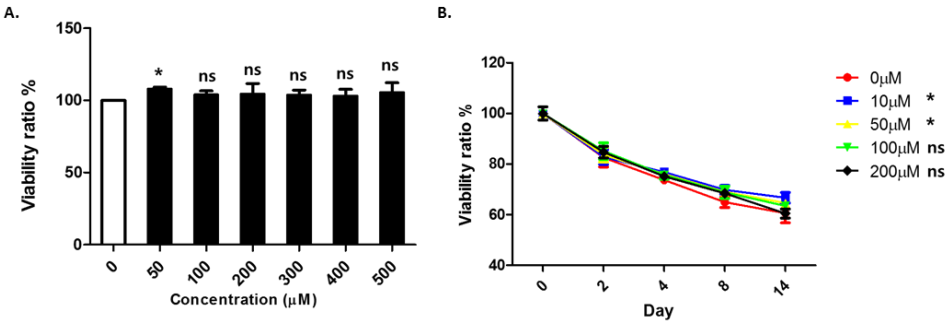

Figure 8. The effect of thiamet G concentrations and incubation time on cell viability. (A) Measurement of cell viability according to thiamet G concentration. Equal numbers of rituximab producing stable cells were seeded to 96-well plates and treated with thiamet G (0, 50, 100, 200, 300, 400, 500 μM) on 30℃. After 4 days, cell viability was measured by CellTiter-Glo assay. (B) Measurement of cell viability

according to the thiamet G treatment incubation periods. Equal numbers of rituximab producing stable cells were seeded to 96-well plates and treated with thiamet G (0, 10, 50, 100, 200 μM) on 30℃. After each time points, cell viability was measured by CellTiter-Glo assay.

9. Thiamet G also improves the production of anti-PD1 antibodies

From the previous results, mass spectrometry confirmed the occurrence of O-GlcNAc on serine 7, serine 12, and serine 14 of the rituximab light chain. Among them, it was found that the production amount was regulated by O-GlcNAc of serine 12. We were wondering if other therapeutic antibodies were affected by O-GlcNAcylation and by thiamet G. Therefore, as a result of aligning the light chain sequences of the anti-PD1 antibodies and rituximab, we found that seine 12 of anti-PD1 antibody was also conserved (Fig. 8A).

After treating 50 μM thiamet G to nivolumab and pembrolizumab stable cells 48 hour later, sup was harvested and immunoblot was performed. As a result, it was confirmed that both production of nivolumab and pembrolizumab increased in the amount of rituximab (Fig. 8B).

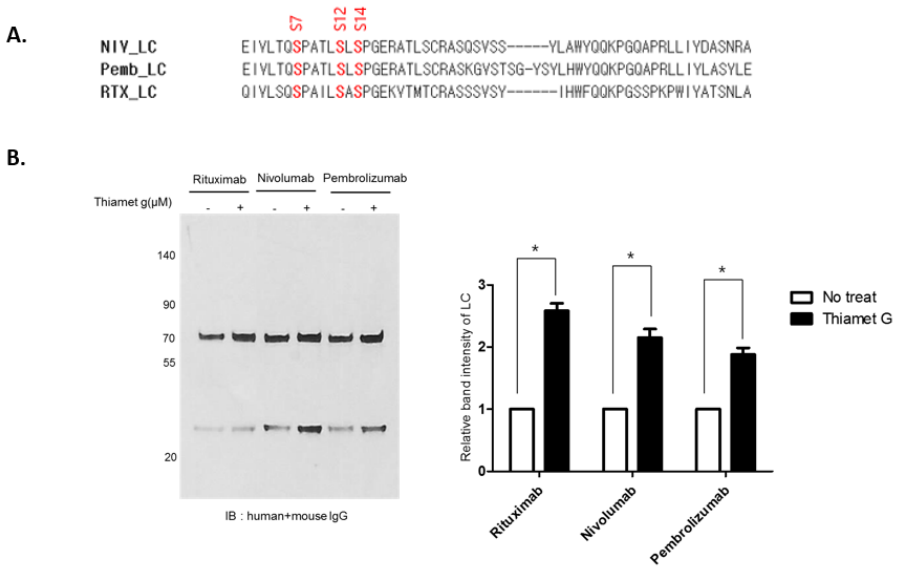

Figure 9. Thiamet G treatment increases the production of anti-PD1 antibodies. (A) Aligned the amino acid sequence of rituximab, nivolumab and pembrolizumab. (B) Equal numbers of rituximab, nivolumab and pembrolizumab producing stable cells were seeded to culture plates and treated with 50 μM thiamet G. After 48 hours, equal volumes of the culture medium (15 μL) was used for immunoblotting with HRP-conjugated anti-human IgG and anti-mouse IgG antibodies. (C) Summary graph after quantification of band intensity of immunoblot depicted in B.

10.Thiamet G treatment decreases O-GalNAc modification of rituximab

O - glycosylation occurring in mammalian cells have O-linked N-acetyl-galactosamine modifications. N-acetyl-galactosamine (O-GalNAc) connected to serine and threonine, in addition to O-GlcNAc.[32] The salvage pathway of O-GalNAc and O-GlcNAc is known to cause cross-talk, thus we assumed that thiamet G treatment might affect the formation of O-GalNAc as well as O-GlcNAc. Thus, lectin binding assay of purified rituximab was performed to thiamet G treated rituximab using Jacalin, which is known to bind to O-GalNAc (Fig. 9A, left panel). Thiamet G treated rituximab showed a decrease in O-GalNAcylation compared to no treated rituximab. Human IgA was reported to cause O - GalNAc in the hinge region and was used as a positive control for the Jacalin binding assay. The right panel of Fig. 9A was re-blotted to confirm that quantification of rituximab is equivalent.

Next, we conducted a mass spectrometry analysis by LTQ-Orbitrap-mass spectrometer to analyse the O-GalNAc modification of rituximab light chain. As shown in Fig. 9B, we found 7 sites of O-GalNAc modified residues and the O-GalNAc modification of thiamet G treated rituximab was reduced compared to no treated rituximab in 5 of 7 residues.

A.

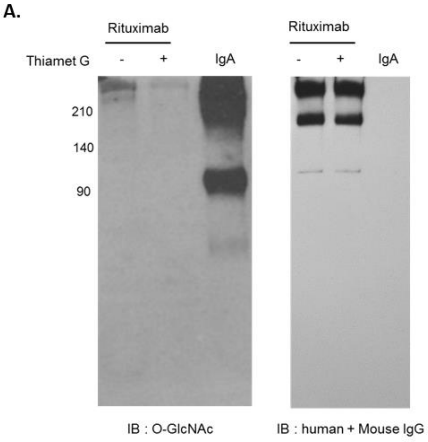

B.

	Num.	S/T	Relative composition% NT	TMG
	42	S	9.1	18.2
*	51	S	11.8	5.9
*	55	S	41.2	5.9
	91	T	4.3	5.3
*	101	T	30.4	15.8
*	155	S	7.7	4.4
*	181	S	6.2	5.3

Figure 10. Thiamet G decreases the heterogeneity of O-GalNAc modification on rituximab. (A) O-GalNAcylation of rituximab is decreased upon thiamet G treatment in non-reducing condition. Left panel: Purified rituximab (1 μg) were immunoblotted with biotinylated Jacalin and HRP conjugated streptavidin. Human IgA was used as positive control for Jacalin binding assay. Right panel: re-blotted with HRP-conjugated anti-human IgG and anti-mouse IgG antibodies for rituximab quantification. (B) An MS/MS spectrum was generated from LTQ-orbitrap-mass spectrometer. Detected O-GalNAc glycosylation on rituximab light chain and the relative composition. Asterisks (red) represent the thiamet G treated rituximab residues which show the low O-GalNAc composition compared to no treated rituximab.

11. Thiamet G does not work on transiently expressed rituximab on CHOK-1 cells

We have tried several times to demonstrate the effect of thiamet G by transiently expressing rituximab in CHO-K1 cells rather than in stable cells. However, the effect of thiamet G on the transient expression system could not be ascertained. In left panel of Fig. 10A, CHO-K1 cells were pre-treated with 0, 10, 30, 50, 100 μM thiamet G for 2 hours and then transiently expressed at the same ratio of heavy chain and light chain. As a result of confirming the transient expression of the rituximab after 48 hours, unlike the result of rituximab stable cell (Fig.10A, right panel), transient production of rituximab did not increase even if the concentration of thiamet G was increased.

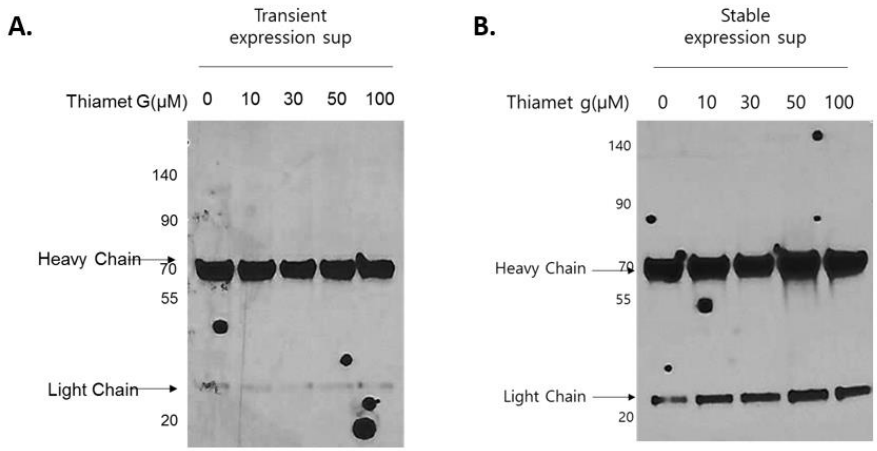

Figure 11. Thiamet G does not show the production increase in transient expression system. Transiently expressed rituximab in CHO-K1 cells (A) and rituximab expressed in stable cells (B) with thiamet G treatments. Pre-treat the thiamet G on 0, 10, 30, 50, 100 μM concentration for 2 hours. Light and heavy chains were transfected to CHO-K1 cells at the same ratio. Then incubated at 37℃ for 48 hours. Rituximab stable cells were also incubated at the same conditions. Harvested

sup were subjected to immunoblot with human and mouse IgG specific-HRP conjugated antibody.

IV. DISCUSSION

We developed a new and improved technology to increase production efficiency and reduce production cost, by doubling the yield of rituximab using thiamet G. The rituximab produced by thiamet G treatment does not show any changes in its CDC or ADCC and protein thermal stability compared to rituximab produced under normal conditions. Therefore, this technology is applicable for rituximab biosimilar production.

Developing OGA knockout cell lines could be an alternative approach to increase production rates. Unfortunately, OGA knockout cells show significantly reduced proliferation rate than wild-type cells.[33] Moreover, the decreased genome stability of OGA cells implies the difficulty of maintaining a healthy cell line to produce rituximab.[33] Therefore, at present, it is most cost-effective to select a drug with a low unit price among the OGA-specific inhibitors, such as thiamet G, to increase the production of rituximab.

The results in Figure 1 and 2 show that the expression levels of both heavy and light chains are affected by thiamet G and both light and heavy chains of rituximab were O-GlcNAcylated in Figure 3A and 4A. These results suggest that O-GlcNAc modification may not only occur in the light chains, but also in the heavy chains. However, in the protein mass spectrometry we only found O-GlcNAcylated sites in the light chain of rituximab produced by thiamet G-treated cells. Currently, we cannot explain why only the light chain sites were detected.

There are several difficulties in studying O-GlcNAcylation. For instance O-GlcNAc modified peptides are not readily detected in most mass spectrometers for two reasons.[34] First, the β-O-glycosidic bond is highly labile.[35] Second, since O-glycosylation by O-GalNAc and O-GlcNAc occurs in various forms, it is difficult to

detect the molecular weight of the attached peptides at a constant value.[34] To overcome the difficulties of proving O-GlcNAcylation of rituximab through mass spectrometry, we demonstrated the presence of O-GlcNAc in two ways. In the immunoblot analysis using the highly functional O-GlcNAc antibody, which is used with most O-GlcNAc proteins, we show that O-GlcNAc binds not only to commercially available Mabthera but also to the rituximab produced in our CHO cells (Fig. 2A). Furthermore, we demonstrate the increased O-GlcNAc level upon thiamet G treatment.

Meanwhile, thiamet G treatment in Fig3A shows only slight difference. For this reason, what we are thinking is that rituximab is synthesized and O-GlcNAc occurs abundantly in intracellular processing, but it is cleaved by hexosaminidase via secretory pathways, ER, golgi complex and cytoplasm. As a basis for this hypothesis, we compared the levels of O-GlcNAc by thiamet G in purified rituximab (Fig. 3) and the rituximab inside of cells respectively (data not shown), and we found that rituximab inside of cell showed a much higher O - GlcNAc level by thiamet G than secreted rituximab. Furthermore, O-GlcNAc of rituximab which was confirmed by mass spectrometry and western blot might be O-GlcNAc of rituximab that came out from dead cells. We are currently conducting further research on this.

We also investigated the mechanism by which O-GlcNAcylation increases the protein stability of rituximab. In several proteins, O-GlcNAcylation has been emphasised to be one of the signal transduction processes that changes the signalling process by phosphorylation,[36] due to its competitive binding property to serine/threonine.[34] In addition, binding of O-GlcNAc induces deformation of certain amino acid motifs, leading to changes in protein function, such as the nuclear localisation signal associated with protein nuclear transfer[37] or transcription factors bound to DNA.[17,38] On the other hand, non-specific O-GlcNAcylation processes are also known.[15] Some proteins, such as nuclear pore protein,[39,40] specificity protein1 (Sp1),[18,19,41] Forkhead box protein O1 (FOXO1),[42,43] and Tau[44] have been reported to

exhibit severe O-GlcNAcylation. This mechanism is related to the characteristics of OGT, which preferentially reacts to substrates with flexible elements. The production of most of these proteins, such as Sp1, nuclear pore protein, and Tau was increased by thiamet G treatment. Similar to these proteins, the O-GlcNAcylation of rituximab appears to be similar to the mechanism by which Sp1 protein stability is increased by O-GlcNAcylation. It has been reported that Sp1 is a protein that becomes O-GlcNAcylated, which increases its protein stability.[18] It has also been shown that O-GlcNAcylation increases protein stability of nascent peptides during Sp1 protein translation.[19] It was thus suggested that O-GlcNAcylation of the nascent peptide would inhibit ubiquitylation and proteasomal degradation of the protein under production, resulting in increased protein stability. The fact that OGT was attached to an early known ribosome,[45] suggests that many proteins could be O-GlcNAcylated by OGT during the polypeptide elongation process. The O-glycosylation of rituximab is also expected to increase protein stability by the same mechanism as for Sp1, and further biochemical experiments are required to prove this.

Glycosylation of antibodies is an important determinant of their quality and plays an important role in therapeutic antibodies.[46] Therefore, it is important to control the quality of the drug when producing it, so that the glycan is uniformly attached in each batch.[46] International conventions on harmonisation (ICH) guidance examines the heterogeneity of oligosaccharides and require evidence that each batch is reproducible.[47] However, there is no need for research and monitoring of O-glycosylation, as they are limited to N-glycans for which various analytical methods are present. Retention of O-GlcNAc by thiamet G may possibly contribute to greatly simplifying the structure of the oligosaccharide by inhibiting the binding of O-GlcNAc. In CHO, a wide variety of O-type oligosaccharides have been reported to exist.[48] OGT firstly acts on Ser-like O-Glc residues, resulting in the extension of oligosaccharides in the presence of COSMC chaperones.[49] The O-GlcNAcylation of rituximab suggests the possibility of also O-GalNAcylation, although reports on

competition among two types of O-glycosylation are lacking. However, if the analytical technology is established to differentiate between O-GlcNAc and O-GalNAc, the role of thiamet G in modulating attachment of each oligosaccharide can be determined. Currently, few analytical methods for O-type oligosaccharides has been established, and studies of O-type oligosaccharides are very difficult. However, efforts like ours, will contribute to the analysis of O-type oligosaccharides and open up the control field of this oligosaccharide.

V. CONCLUSION

In this study, we found that the rituximab is an O-GlcNAcylated protein, and also the production of rituximab could be increased by thiamet G treatment, which reduces the protein degradation of rituximab

The O-GlcNAc of the rituximab is presumed to occur in both the heavy chain and the light chain. And it is evident that the O-GlcNAc of serine 12 on the light chain critically affects the productions. Treatment of thiamet G increased the production of anti-PD1 antibodies which also have serine 12 on the light chain as well as rituximab. Therefore, we suggest that O-GlcNAcylation of serine12 by treatment with thiamet G could be used as a way to increase the production of rituximab and antibodies with serine 12.

REFERENCES

1. Tedder TF, Klejman G, Disteche CM, Adler DA, Schlossman SF, Saito H. Cloning of a complementary DNA encoding a new mouse B lymphocyte differentiation antigen, homologous to the human B1 (CD20) antigen, and localization of the gene to chromosome 19. J Immunol 1988;141:4388-94.

2. McLaughlin P, Grillo-Lopez AJ, Link BK, Levy R, Czuczman MS, Williams ME, et al. Rituximab chimeric anti-CD20 monoclonal antibody therapy for relapsed indolent lymphoma: half of patients respond to a four-dose treatment program. J Clin Oncol 1998;16:2825-33.

3. Arnold JN, Wormald MR, Sim RB, Rudd PM, Dwek RA. The impact of glycosylation on the biological function and structure of human immunoglobulins. Annu Rev Immunol 2007;25:21-50.

4. Audagnotto M, Dal Peraro M. Protein post-translational modifications: In silico prediction tools and molecular modeling. Comput Struct Biotechnol J 2017;15:307-19.

5. Van den Steen P, Rudd PM, Dwek RA, Opdenakker G. Concepts and principles of O-linked glycosylation. Crit Rev Biochem Mol Biol 1998;33:151-208.

6. Subedi GP, Barb AW. The Structural Role of Antibody N-Glycosylation in Receptor Interactions. Structure 2015;23:1573-83.

7. Mossner E, Brunker P, Moser S, Puntener U, Schmidt C, Herter S, et al. Increasing the efficacy of CD20 antibody therapy through the engineering of a new type II anti-CD20 antibody with enhanced direct and immune effector cell-mediated B-cell cytotoxicity. Blood 2010;115:4393-402.

8. Peipp M, Lammerts van Bueren JJ, Schneider-Merck T, Bleeker WW, Dechant M, Beyer T, et al. Antibody fucosylation differentially impacts cytotoxicity mediated by NK and PMN effector cells. Blood 2008;112:2390-9.

9. Monnet C, Jorieux S, Souyris N, Zaki O, Jacquet A, Fournier N, et al. Combined glyco- and protein-Fc engineering simultaneously enhance cytotoxicity and half-life of a therapeutic antibody. MAbs 2014;6:422-36.

10. Ishino T, Wang M, Mosyak L, Tam A, Duan W, Svenson K, et al. Engineering a monomeric Fc domain modality by N-glycosylation for the half-life extension of biotherapeutics. J Biol Chem 2013;288:16529-37.

11. Gu J, Lei Y, Huang Y, Zhao Y, Li J, Huang T, et al. Fab fragment glycosylated IgG may play a central role in placental immune evasion. Hum Reprod 2015;30:380-91.

12. Wopereis S, Lefeber DJ, Morava E, Wevers RA. Mechanisms in protein O-glycan biosynthesis and clinical and molecular aspects of protein O-glycan biosynthesis defects: a review. Clin Chem 2006;52:574-600.

13. Hanisch FG. O-glycosylation of the mucin type. Biol Chem 2001;382:143-9.

14. Bennett EP, Mandel U, Clausen H, Gerken TA, Fritz TA, Tabak LA. Control of mucin-type O-glycosylation: a classification of the polypeptide GalNAc-transferase gene family. Glycobiology 2012;22:736-56.

15. Yang X, Qian K. Protein O-GlcNAcylation: emerging mechanisms and functions. Nat Rev Mol Cell Biol 2017;18:452-65.

16. Hart GW, Housley MP, Slawson C. Cycling of O-linked beta-N-acetylglucosamine on nucleocytoplasmic proteins. Nature 2007;446:1017-22.

17. Housley MP, Rodgers JT, Udeshi ND, Kelly TJ, Shabanowitz J, Hunt DF, et al. O-GlcNAc regulates FoxO activation in response to glucose. J Biol Chem 2008;283:16283-92.

18. Han I, Kudlow JE. Reduced O glycosylation of Sp1 is associated with increased proteasome susceptibility. Mol Cell Biol 1997;17:2550-8.

19. Zhu Y, Liu TW, Cecioni S, Eskandari R, Zandberg WF, Vocadlo DJ. O-GlcNAc occurs cotranslationally to stabilize nascent polypeptide chains. Nat Chem Biol 2015;11:319-25.

20. Zhang F, Su K, Yang X, Bowe DB, Paterson AJ, Kudlow JE. O-GlcNAc modification is an endogenous inhibitor of the proteasome. Cell 2003;115:715-25.

21. Wang J, Torii M, Liu H, Hart GW, Hu ZZ. dbOGAP - an integrated bioinformatics resource for protein O-GlcNAcylation. BMC Bioinformatics 2011;12:91.

22. Yuzwa SA, Macauley MS, Heinonen JE, Shan X, Dennis RJ, He Y, et al. A potent mechanism-inspired O-GlcNAcase inhibitor that blocks phosphorylation of tau in vivo. Nat Chem Biol 2008;4:483-90.

23. Ortiz-Meoz RF, Jiang J, Lazarus MB, Orman M, Janetzko J, Fan C, et al. A small molecule that inhibits OGT activity in cells. ACS Chem Biol 2015;10:1392-7.

24. Lee JW, Heo W, Lee J, Jin N, Yoon SM, Park KY, et al. The B cell death function of obinutuzumab-HDEL produced in plant (Nicotiana benthamiana L.) is equivalent to obinutuzumab produced in CHO cells. PLoS One 2018;13:e0191075.

25. Laughlin ST, Bertozzi CR. Metabolic labeling of glycans with azido sugars and subsequent glycan-profiling and visualization via Staudinger ligation. Nat Protoc 2007;2:2930-44.

26. Vocadlo DJ, Hang HC, Kim EJ, Hanover JA, Bertozzi CR. A chemical approach for identifying O-GlcNAc-modified proteins in cells. Proc Natl Acad Sci U S A 2003;100:9116-21.

27. Boyd PN, Lines AC, Patel AK. The effect of the removal of sialic acid, galactose and total carbohydrate on the functional activity of Campath-1H. Mol Immunol 1995;32:1311-8.

28. Shinkawa T, Nakamura K, Yamane N, Shoji-Hosaka E, Kanda Y, Sakurada M, et al. The absence of fucose but not the presence of galactose or bisecting N-acetylglucosamine of human IgG1 complex-

type oligosaccharides shows the critical role of enhancing antibody-dependent cellular cytotoxicity. J Biol Chem 2003;278:3466-73.

29. Herter S, Herting F, Mundigl O, Waldhauer I, Weinzierl T, Fauti T, et al. Preclinical activity of the type II CD20 antibody GA101 (obinutuzumab) compared with rituximab and ofatumumab in vitro and in xenograft models. Mol Cancer Ther 2013;12:2031-42.

30. Mimura Y, Church S, Ghirlando R, Ashton PR, Dong S, Goodall M, et al. The influence of glycosylation on the thermal stability and effector function expression of human IgG1-Fc: properties of a series of truncated glycoforms. Mol Immunol 2000;37:697-706.

31. Sola RJ, Griebenow K. Effects of glycosylation on the stability of protein pharmaceuticals. J Pharm Sci 2009;98:1223-45.

32. Hurtado-Guerrero R. Recent structural and mechanistic insights into protein O-GalNAc glycosylation. Biochem Soc Trans 2016;44:61-7.

33. Yang YR, Song M, Lee H, Jeon Y, Choi EJ, Jang HJ, et al. O-GlcNAcase is essential for embryonic development and maintenance of genomic stability. Aging Cell 2012;11:439-48.

34. Hart GW, Slawson C, Ramirez-Correa G, Lagerlof O. Cross talk between O-GlcNAcylation and phosphorylation: roles in signaling, transcription, and chronic disease. Annu Rev Biochem 2011;80:825-58.

35. Zachara NE. Detecting the "O-GlcNAc-ome"; detection, purification, and analysis of O-GlcNAc modified proteins. Methods Mol Biol 2009;534:251-79.

36. Yang WH, Kim JE, Nam HW, Ju JW, Kim HS, Kim YS, et al. Modification of p53 with O-linked N-acetylglucosamine regulates p53 activity and stability. Nat Cell Biol 2006;8:1074-83.

37. Seo HG, Kim HB, Kang MJ, Ryum JH, Yi EC, Cho JW. Identification of the nuclear localisation signal of O-GlcNAc transferase and its nuclear import regulation. Sci Rep 2016;6:34614.

38. Ji S, Park SY, Roth J, Kim HS, Cho JW. O-GlcNAc modification of PPARgamma reduces its transcriptional activity. Biochem Biophys Res Commun 2012;417:1158-63.

39. Li B, Kohler JJ. Glycosylation of the nuclear pore. Traffic 2014;15:347-61.

40. Zhu Y, Liu TW, Madden Z, Yuzwa SA, Murray K, Cecioni S, et al. Post-translational O-GlcNAcylation is essential for nuclear pore integrity and maintenance of the pore selectivity filter. J Mol Cell Biol 2016;8:2-16.

41. Su K, Roos MD, Yang X, Han I, Paterson AJ, Kudlow JE. An N-terminal region of Sp1 targets its proteasome-dependent degradation in vitro. J Biol Chem 1999;274:15194-202.

42. Eijkelenboom A, Burgering BM. FOXOs: signalling integrators for homeostasis maintenance. Nat Rev Mol Cell Biol 2013;14:83-97.

43. Fardini Y, Perez-Cervera Y, Camoin L, Pagesy P, Lefebvre T, Issad T. Regulatory O-GlcNAcylation sites on FoxO1 are yet to be identified. Biochem Biophys Res Commun 2015;462:151-8.

44. Hastings NB, Wang X, Song L, Butts BD, Grotz D, Hargreaves R, et al. Inhibition of O-GlcNAcase leads to elevation of O-GlcNAc tau and reduction of tauopathy and cerebrospinal fluid tau in rTg4510 mice. Molecular Neurodegeneration 2017;12:39.

45. Zeidan Q, Wang Z, De Maio A, Hart GW. O-GlcNAc cycling enzymes associate with the translational machinery and modify core ribosomal proteins. Mol Biol Cell 2010;21:1922-36.

46. Schiestl M, Stangler T, Torella C, Cepeljnik T, Toll H, Grau R. Acceptable changes in quality attributes of glycosylated biopharmaceuticals. Nat Biotechnol 2011;29:310-2.

47. Zhang P, Woen S, Wang T, Liau B, Zhao S, Chen C, et al. Challenges of glycosylation analysis and control: an integrated approach to producing optimal and consistent therapeutic drugs. Drug Discov Today 2016;21:740-65.

48. Yang Z, Halim A, Narimatsu Y, Jitendra Joshi H, Steentoft C, Schjoldager KT, et al. The GalNAc-type O-Glycoproteome of CHO cells characterized by the SimpleCell strategy. Mol Cell Proteomics 2014;13:3224-35.

49. Wang Y, Ju T, Ding X, Xia B, Wang W, Xia L, et al. Cosmc is an essential chaperone for correct protein O-glycosylation. Proc Natl Acad Sci U S A 2010;107:9228-33.

ABSTRACT (in Korean)

Thiamet G를 이용한 O-GlcNAc결합에 의한 리툭시맵의 생산량 증가

<지도교수 김 주 영>

연세대학교 대학원 의과학과

김 혜 연

O-형 당사슬 결합은 CHO세포에서 생성된 재조합 단백질에서 발생하지만, 이 현상은 광범위하게 연구되지 않았다. 본 연구는 리툭시맵이 O-형 당사슬결합인 N-acetyl-glucosamine (O-GlcNAc)이 결합하는 단백질이라는 것을 처음으로 규명하였다.

리툭시맵에는 O-GlcNAc이 결합하는 아미노산인 세린과 트레오닌이 풍부하게 존재하는데, O-GlcNAcase (OGA)의 억제제인 thiamet G를 처리하는 경우 생산량이 두배로 증가하고 반대로 O-GlcNAc 전이 효소 (OGT)를 억제 하였을 때는 생산량이 감소하였다. ^{35}S 메타이오닌을 이용한 단백안정성 실험에서 thiamet G를 처리했을 때 rituximab의 단백안정성이 증가하는 것으로 나타났다. O-GlcNAc-특이적 항체를 이용해 thiamet G 처리에 의해 리툭시맵의 O-GlcNAc결합 증가를 확인하였고, N-acetyl-azido-glucosamine (Ac4GlcNAz)을 사용한

메타볼릭 라벨링을 통해 리툭시맵이 O-GlcNAc 결합하는단백임을 재확인하였다. 단백질 질량분석으로, 리툭시맵 경쇄의 세린 7, 12 및 14는 O-GlcNAc이 결합함을 발견하였는데 그 중 S12A 돌연변이는 리툭시맵의 안정성을 감소시켰을 뿐 아니라 thiamet G에 의한 생산량 증가를 보이지 않는 결과를 보여 12번 세린의 O-GlcNAc 결합이 rituximab의 단백안정성을 통한 생산량 조절에 중요한 부위임을 규명하였다. 세포 독성 및 열 안정성 분석을 통해 thiamet G를 처리하여 생산한 리툭시맵의 생물학적 및 물리적 특성에 차이가 없음을 확인함으로써 thiamet G 처리는 리툭시맵의 기능을 크게 변경시키지 않고 생산성을 향상시킬 수 있는 효과적인 방법임을 증명하였다. 한편, 경쇄의 12번 세린은 2종의 항 PD1 항체에서 보존되어 있을 뿐 아니라 이들 2종의 항체 역시 thiamet G에 의한 생산이 증가함을 발견하였다.

이상의 결과는 thiamet G의 처리에 의한 세린12의 O-GlcNAc결합은 리툭시맵 및 세린12를 갖는 항체들의 생산량을 증가시키는 방법으로 사용 될 수 있음을 시사한다.

핵심되는 말: 리툭시맵, O-GlcNAc, 생산 수율, Thiamet G, ADCC, CDC, 열 안정성